

# Interactive Dissection of Digital Organs Based on Metaballs

Junjun Pan<sup>\*</sup>  
State Key Laboratory of Virtual  
Reality Technology and  
Systems  
Beihang University  
Beijing, China  
junjunpan@gmail.com

Shizeng Yan  
State Key Laboratory of Virtual  
Reality Technology and  
Systems  
Beihang University  
Beijing, China  
726819721@qq.com

Hong Qin  
Department of Computer  
Science  
Stony Brook University (SUNY  
Stony Brook)  
New York, USA  
qin@cs.stonybrook.edu

## ABSTRACT

This paper describes an interactive dissection approach based on metaballs for digital organs in virtual surgery. For organ's geometry, we employ a novel hybrid model comprising both inner metaballs and high-resolution surface mesh with texture. Using metaballs, the organ interior is geometrically simplified via a set of overlapping spheres with different radii. For physical representation, we present a hybrid framework to interlink metaballs with moving least squares (MLS) based meshfree method. MLS enables the direct and rapid transition from metaballs to local nodal formulations in physical modeling. For soft tissue dissection, the nature of our MLS-driven meshfree method also facilitates adaptive topology modification and cutting surface reconstruction. As nodal points only exist temporarily in localized regions adjacent to the cutting path, our method could generate accurate cutting surface without sacrificing real-time computational efficiency.

## CCS Concepts

• **Computing methodologies** → **Computer graphics**; *Graphics systems and interfaces*; Virtual reality; Shape modeling;

## Keywords

Metaballs; Dissection; Meshfree; Virtual Surgery

## 1. INTRODUCTION

With the progresses of virtual reality technologies being made in medical fields, VR-based surgical simulation has attracted increasing research interests in recent years [11, 12]. The key techniques involves physical deformation of organs

<sup>\*</sup>Dr. Pan is the corresponding author.

Permission to make digital or hard copies of all or part of this work for personal or classroom use is granted without fee provided that copies are not made or distributed for profit or commercial advantage and that copies bear this notice and the full citation on the first page. Copyrights for components of this work owned by others than ACM must be honored. Abstracting with credit is permitted. To copy otherwise, or republish, to post on servers or to redistribute to lists, requires prior specific permission and/or a fee. Request permissions from [permissions@acm.org](mailto:permissions@acm.org).

CGI2016, June 28th-July 1st, 2016, Heraklion, Crete, Greece

© 2016 ACM. ISBN 123-4567-24-567/08/06...\$15.00

DOI: 10.475/123\_4

and simulation of basic surgical procedures, such as dissection. In this paper, we present an interactive dissection approach for digital organs by combing the geometry of metaballs with physically-accurate meshfree method. For organ geometry, we employ a novel hybrid model comprising both inner metaballs and fine surface mesh with texture. Using metaballs, the organ interior can be approximated by a set of coarse, overlapping spheres with different radii. Moreover, if metaballs are equipped with any type of physical properties, the metaballs could also participate in the global deformation of organ enabled by position based dynamics (PBD). For organs' physical representation, we choose the meshfree method due to its natural advantages in cutting simulation. Here we generate a hybrid framework to interlink metaballs with physics-driven meshfree method based on moving least squares (MLS) shape functions. It enables the direct transition from metaballs to local nodal formulations, which afford potential-energy-correct physical modeling and simulation over continuum domain with physical accuracy. For the coupling of local nodal points and metaballs nearby, we utilize the stretching potential energy and displacement to transfer the motion between these two different systems. For soft tissue dissection, the nature of our MLS-driven meshfree method supports adaptive topology modification and cutting surface reconstruction. Finally, once dissection is completed, the separated nodal points are converted back into the new overlapping spheres by the scheme of Centroid Voronoi Diagram. And the cutting surface is reconstructed from the down-sampled nodal points by the Constraint Delaunay Triangulation. In our method, as nodal points only exist temporarily in localized regions adjacent to the cutting path, it could generate accurate cutting surface without sacrificing real-time computational efficiency.

## 2. RELATED WORK

In principle, deformation and cutting simulation methods can be classified into four different categories.

**Finite element methods (FEM).** FEM can perform accurate deformation result but with high computation cost. Cueto et al. [4] gave a survey of the latest progress of FEM research and their application in virtual surgery. Generally, FEM-based dissection faces the challenges in realistic cutting surface reconstruction and dynamic topological update [5].

**Mass-spring based methods.** This type of methods

simplify the physical structure of objects as mass points and linked springs. It can achieve high computation efficiency, but with the sacrifice of physical accuracy. Pan et al. [12] presented a multi-layer mass spring model to simulate the membrane tissue dissection in laparoscopic intestine surgery.

**Meshfree methods.** Meshfree methods are also called meshless methods, in which the physical behaviors are driven by material distance-based radial functions [10]. These approaches do not require any explicit topological construction. Thus they can offer great flexibility in accommodating topological changes when confronting cutting simulation. Jones et al. [6] presented a meshfree method to deform elastoplastic object. Adams et al. [1] comprehensively discussed the meshless methods for physics-based modeling and simulation. However, meshfree method is not without limitations. When the globally arbitrary cutting of organs happens, its computation cost will drastically increase due to the time-consuming modification of global material distance field.

**Position-based dynamics (PBD)** is another widely used method in physical deformation, due to its fast, robustness and position based manipulation feature [2]. Pan et al. [11] presented an interactive dissection approach for hybrid soft tissue models, which contain both surface mesh and tetrahedra, by extended position-based dynamics. Müller et al. [9] applied the PBD framework to simulate soft objects in real-time environment.

Quite different from above physical modeling methods, most existing metaballs-based approaches focus on the geometric modeling using implicit surface [15]. In 2015, Pan et al. [14] presented a deformation approach for organs using metaballs. Its novelty hinges upon the integration of metaballs and PBD which enables metaballs-based organs to deform dynamically. Based on their research, our work is to interlink metaballs with physically-accurate meshfree method, and present a hybrid framework for dissection simulation.

### 3. OVERVIEW

The dissection process can be illustrated as Figure 1. When the scalpel moving across the spheres in metaballs model, the dissected spheres will be removed and converted into the nodal points. The movement of these points are driven by moving least squares shape functions, and it should also couple with the deformation of spheres nearby. When the scalpel leaves the soft tissue, these points will be separated and converted back into spheres. The system consists of following key components:

**Hybrid geometric model.** A hybrid geometric model, comprising both surface mesh and the metaballs, is employed to represent the digital organs. The finer surface mesh with high-resolution geometric information and texture, represents the boundary structure of organs. Through the use of metaballs, the organ interior is geometrically simplified via a set of coarse, overlapping spheres with different radii.

**Global deformation.** Position-based dynamics (PBD) is utilized to compute the position of sphere centers for organs global deformation. To preserve the local detail of the metaballs, we add the Laplacian coordinates constraints to update the position of sphere centers. Then the local volume preservation is employed to adjust the radii of spheres. Finally, an automatic skinning algorithm is presented to map

the deformation to the surface mesh in real time.

**Dissection simulation.** During cutting, the dissected spheres will be removed and converted into the nodal points. The movement of these points are driven by moving least squares meshfree method and coupled with the deformation of spheres nearby. When dissection finished, these points will be separated and converted back into spheres with updated topology connection.

## 4. CONSTRUCTION OF METABALLS AND DEFORMATION

We use Sphere Tree Construction Toolkit [3] to pack the spheres in the triangular mesh of organs. The key strategy of this toolkit is to find the medial surface of an object using the Voronoi Diagram and pack spheres to approximate the objects. Then a series of optimization strategies are employed to adjust the spheres radii, fill the vacant space and merge the extremely overlapping spheres. Finally, a global electrostatic attraction model [14] is proposed to drive the metaballs best matching the boundary of organ mesh.

After the construction of metaballs topology, the position based dynamics (PBD) is employed to compute the position of sphere centers. Considering the irregular topology of metaballs model, we only apply stretching constraints for the deformation of metaballs. The constraint function about stretch can be described as follows:

$$C_{stretching}(\vec{p}_1, \vec{p}_2) = |\vec{p}_1 - \vec{p}_2| - d, \quad (1)$$

where  $d$  is the initial distance between sphere centers  $\vec{p}_1$  and  $\vec{p}_2$  before simulation.

Nevertheless, stretching constraints in PBD only make 2D constraints and lacks of constraints in 3D space. So we apply the Laplacian coordinates constraint to preserve the local detail of the metaballs shape. Besides, we design a straightforward method to preserve the local volume of organs by adjusting the spheres radii in the area under surgical instruments interaction. Figure 2(a) illustrates the deformation of metaballs model for the liver by a grasper in minimally invasive surgery.

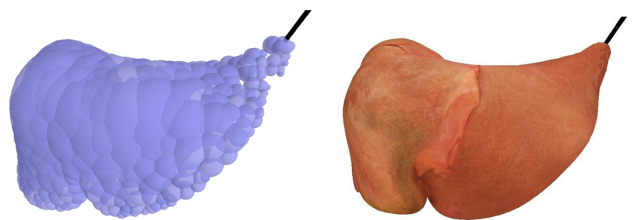


**Figure 2.** The deformation of liver model by metaballs-based method. (a) The metaballs model, (b) The surface mesh with texture.

After the deformation of metaballs, the final task is transforming this deformation to the exterior surface. So we need to construct the mapping between the metaballs and surface mesh of organs. This process is very similar to the skinning technique in the skeleton driven animation [13]. Here we treat the spheres as the "interior skeleton" and the polygon mesh as the "skin". And an automatic algorithm based on distance field function [14] is designed to assign the weights for each vertex in surface mesh. Figure 2(b) illustrates the final deformation result of surface mesh.

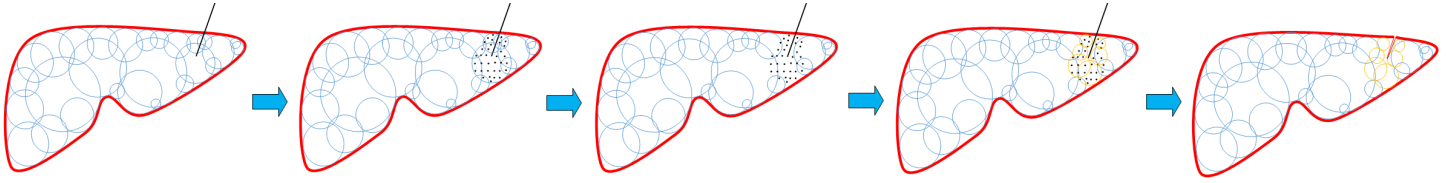


Figure 1. The illustration of our hybrid cutting simulation method.

## 5. DISSECTION SIMULATION

### 5.1 Meshfree Method based on Moving Least Squares

In cutting simulation, we use the nodal points in mesh free method to replace the dissected metaballs, as the local dynamic model. Once the scalpel touching the sphere in metaballs model, this sphere will be removed and converted into the points under uniform sampling. To guarantee the mass conservation, supposing  $m_i$  is the mass of sphere  $i$  and  $n$  is the number of nodal points converted from the sphere  $i$ , the mass of each converted point will be  $m_i/n$ .

To measure the physical effect of a nodal point to its neighborhood, we use following polynomial kernel to compute the mass distribution of this point.

$$\omega_h(r) = \frac{315}{64\pi h^9} \begin{cases} (h^2 - r^2)^3, & 0 \leq r \leq h \\ 0 & , \text{otherwise} \end{cases} \quad (2)$$

Where  $r$  is the distance to the point and  $h$  is the support of the kernel.

In order to compute the strain, stress and the elastic body forces, the spatial derivatives of displacement field  $\nabla \mathbf{u}$  are needed. These derivatives can be estimated from the displacement vectors of neighboring points. Here we employ the moving least squares shape functions to approximate  $\nabla \mathbf{u}$  with a linear basis. The spatial derivatives at the position of point  $\mathbf{x}_i$  can be computed as Eq.(3):

$$\nabla u(\mathbf{x}_i) = \mathbf{A}_i^{-1} \sum_j (u_j - u_i) \omega_{ij}(\|\mathbf{x}_{ij}\|) \mathbf{x}_{ij}, \quad (3)$$

where  $u(\mathbf{x}_i)$  is the x-component  $u$  of the displacement field  $\mathbf{u} = (u, v, w)^T$ .  $\mathbf{x}_{ij}$  is the difference vector between point  $i$  and its neighboring points  $j$ . There is  $\mathbf{x}_{ij} = \mathbf{x}_i - \mathbf{x}_j$ .  $\omega_{ij}$  is the mass weight, which can be computed by Eq.(2), between point  $i$  and  $j$ .  $\mathbf{A}_i$  is the moment matrix, which is only related with the distribution of point  $i$  and its neighboring points.  $\mathbf{A}_i$  can be pre-computed by Eq.(4) and used for the computation of the derivative of  $v$  and  $w$  as well.

$$\mathbf{A}_i = \sum_j \omega_{ij}(\|\mathbf{x}_{ij}\|) \mathbf{x}_{ij} \mathbf{x}_{ij}^T. \quad (4)$$

Using Eq.(3) we can also compute the strain  $\epsilon_i$  and the stress  $\sigma_i$  at point  $i$  by following equations:

$$\epsilon_i = \mathbf{J}_i^T \mathbf{J}_i - \mathbf{I} = \nabla \mathbf{u}_i + \nabla \mathbf{u}_i^T + \nabla \mathbf{u}_i \nabla \mathbf{u}_i^T, \sigma_i = \mathbf{C} \epsilon_i, \quad (5)$$

where  $\mathbf{J}_i$  is the Jacobian matrix of point  $i$ .  $\mathbf{C}$  is a rank four tensor, approximating the constitutive law of the material. Both  $\epsilon_i$  and  $\sigma_i$  are symmetric 3 by 3 tensors. For an isotropic material,  $\mathbf{C}$  is only related with Young's modulus and Poisson's ratio.

According to the continuum mechanics theory, with  $\epsilon_i$  and  $\sigma_i$ , we can estimate the strain energy  $U_i$  stored around point  $i$  by Eq.(6)

$$U_i = \int_{\Omega} u \, d\Omega = \int_{\Omega} \frac{1}{2} (\epsilon_i \cdot \sigma_i) d\Omega = \frac{1}{2} v_i (\epsilon_i \cdot \sigma_i), \quad (6)$$

where  $v_i$  is the rest volume of point  $i$ . The strain energy is a function of the displacement vector  $\mathbf{u}_i$  for point  $i$  and the displacements  $\mathbf{u}_j$  of all its neighbors. Taking the derivative with respect to these displacements, we can compute the force of neighboring points  $j$  and the acceleration of  $\mathbf{a}_i$ . The force acting on point  $i$  is the negative sum of all  $\mathbf{f}_j$  acting on its neighboring points  $j$ .

$$\mathbf{f}_i = - \sum_j \mathbf{f}_j, \mathbf{f}_j = -\nabla_{\mathbf{u}_j} U_i = -v_i \sigma_i \nabla_{\mathbf{u}_j} \epsilon_i. \quad (7)$$

$$\frac{d^2 \mathbf{u}_i}{dt^2} = \mathbf{a}_i = \mathbf{f}_i / m_i. \quad (8)$$

### 5.2 Metaballs and Topology Modification

When the scalpel leaves the surface mesh and cutting stops, the split points set should be converted back into metaballs with a updated topology connection. Our key strategy is to find the **medial points** in the split points set using the Centroid Voronoi Diagram based method [14], and pack new spheres from these **medial points** to approximate the shape of points set roughly. The whole process can be described as Figure 1. Here we classify all the points into three categories. The first is **boundary points** which is near the boundary of group points. The second is **medial points** which is near the medial surface of points in each group. The medial points approximately have the same distance between the boundary points in its local radius area. They can be identified by the Centroid Voronoi Diagram based method. The third is **middle layer points** which is the rest points in each group. Then we equally down-sample the medial points as the center of new packing spheres in each group. The radius of each sphere can be computed by the Euclidean distance between the sphere center and its nearest boundary point.

### 5.3 Cutting Surface Reconstruction

In the surgery simulation, all the displaying information of digital organs, such as texture and lighting, should be rendering on the surface mesh. So the last task for dissection simulation is the reconstruction of cutting surface. As we use meshfree method for cutting, the nodal points near the sweep surface can be used to generate the surface mesh with geometry detail. To lower the data size of new meshes, the points near the sweep surface should be down-sampled. Then we employ the Constraint Delaunay Triangulation [7] to generate the cutting surface meshes for two sides. And

the approach in [8] is employed to generate the texture of cutting surface. Finally, a mapping will be built between the updated metaballs and the cutting surface mesh.

## 6. EXPERIMENTS

We have implemented our dissection simulation technique using OpenGL, CUDA, and OpenHaptics. All the experiments run on a desktop with NVIDIA GeForceGT 630, Intel(R) Core(TM) i7-4790 CPU (3.60GHz, 8 cores), and 8G RAM. Figure 3 illustrates the simulation results at different stages for both the metaballs and surface mesh of liver. The simulation speed is about 56 fps. Since nodal points only exist temporarily in localized regions adjacent to the cutting path, our method could generate accurate cutting surface without sacrificing real-time computational efficiency.

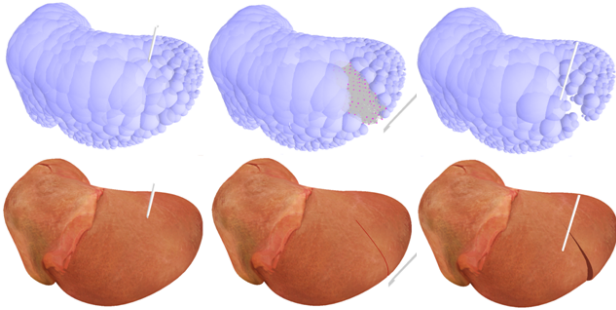


Figure 3. The cutting simulation result of liver.

## 7. CONCLUSIONS

In this paper, we have detailed a interactive dissection approach for digital organs by tight coupling of metaballs and meshfree method. Shape geometry of digital organ consists of both surface mesh and the metaballs, where the fine surface mesh is necessary for the exterior structure of organs, and the interior structure is filled by a set of overlapping spheres. At the physical level, we have demonstrated a hybrid framework that interlinks metaballs with physics-driven meshfree method based on MLS shape functions. MLS approach enables the direct and rapid transformation from metaball geometry to local nodal formulations, participating in physical modeling and simulation over continuum domain with high-fidelity physical realism. For soft tissue dissection, the nature of our MLS-driven meshfree method also facilitates adaptive topology modification and cutting surface reconstruction. Since meshfree methods support the material heterogeneities, in future we plan to extend our dissection method to the soft tissue with different material properties.

## 8. ACKNOWLEDGEMENTS

This research is supported by National Natural Science Foundation of China (No. 61402025, 61532002), National Science Foundation of USA (No. IIS-0949467, 1047715, 1049448) and the Fundamental Research Funds for the Central Universities.

## 9. REFERENCES

[1] B. Adams and M. Wicke. Meshless approximation methods and applications in physics based modeling and animation. In *Eurographics 2009, Tutorial*, 2009.

[2] J. Bender, M. Müller, M. Teschner, and M. Macklin. A survey on position based simulation methods in computer graphics. *Computer Graphics Forum*, 33(6):228–251, 2014.

[3] G. Bradshaw and C. Sullivan. Sphere-tree construction using dynamic medial axis approximation. *Proceedings of the 2002 ACM SIGGRAPH/Eurographics symposium on Computer animation*, pages 33–40, 2002.

[4] E. Cueto and F. Chinesta. Real time simulation for computational surgery: A review. *Advanced Modeling and Simulation in Engineering Sciences*, 1(11):1–18, 2014.

[5] L. Jeřábková, G. Bousquet, S. Barbier, F. Faure, and J. Allard. Volumetric modeling and interactive cutting of deformable bodies. *Progress of Biophysics and Molecular Biology*, 103(2-3):217–224, 2010.

[6] B. Jones, S. Ward, A. Jallepalli, J. Perenia, and A. Bargteil. Deformation embedding for point-based elastoplastic simulation. *ACM Transactions on Graphics*, 33(2):1–9, 2014.

[7] M. Kallmann, H. Bieri, and D. Thalmann. Fully dynamic constrained delaunay triangulations. *Geometric Modeling for Scientific Visualization (Part of the series Mathematics and Visualization)*, pages 241–257, 2011.

[8] X. Li, X. Guo, H. Wang, Y. He, X. Gu, and H. Qin. Meshless harmonic volumetric mapping using fundamental solution methods. *IEEE Transactions on Automation Science and Engineering*, 6(3):409–422, 2009.

[9] M. Macklin, M. Müller, N. Chentanez, and T. Kim. Unified particle physics for real-time applications. *ACM Transactions on Graphics*, 33(4):1–10, 2014.

[10] M. Müller, R. Keiser, A. Nealen, M. Pauly, M. Gross, and M. Alexa. Point based animation of elastic, plastic and melting objects. In *Proceedings of the 2004 ACM SIGGRAPH/Eurographics symposium on Computer animation*, pages 141–151, 2004.

[11] J. Pan, J. Bai, X. Zhao, A. Hao, and H. Qin. Real-time haptic manipulation and cutting of hybrid soft tissue models by extended position-based dynamics. *Computer Animation and Virtual Worlds Volume*, 26(3-4):321–335, 2015.

[12] J. Pan, J. Chang, X. Yang, H. Liang, J. Zhang, T. Qureshi, R. Howell, and T. Hickish. Virtual reality training and assessment in laparoscopic rectum surgery. *The International Journal of Medical Robotics and Computer Assisted Surgery*, 11(2):194–209, 2015.

[13] J. Pan, X. Yang, X. Xie, P. Willis, and J. Zhang. Automatic rigging for animation characters with 3d silhouette. *Computer Animation and Virtual Worlds*, 20(2-3):121–131, 2009.

[14] J. Pan, C. Zhao, X. Zhao, A. Hao, and H. Qin. Metaballs-based physical modeling and deformation of organs for virtual surgery. *The Visual Computer*, 31(6):947–957, 2015.

[15] Y. Wei, S. Cotin, and J. Dequidt. A (near) real-time simulation method of aneurysm coil embolization. *Aneurysm*, 8(29):223–248, 2012.